EVALUATION OF LIQUID DOPING METHODS FOR USE IN LASER POWDER BED FUSION

T. M. Davis* and N. B. Crane*

*Department of Mechanical Engineering, Brigham Young University, Provo, UT 84602

Abstract

Laser powder bed fusion (LPBF) is an additive manufacturing (AM) process that is well known for its geometric versatility and high-quality parts. While the properties of LPBF parts are commonly superior to those made using other AM techniques, LPBF is generally limited to a single material in any given build. While LPBF can accommodate the integration of multiple components into a single part geometrically, the material limitation leads to over-designing to ensure that every component can complete their various functions. Some studies have shown potential methods of 3D composition control throughout a part, but these methods are subject to high cost increases due to build time increases and decreased powder recyclability. A new approach to multi-material LPBF uses liquid dopants to alter the composition in location-specific areas. The current study evaluates two different liquid deposition methods – direct write and inkjet deposition – in relation to their adaptability and utility in LPBF. Inkjet deposition is shown to have significant benefits compared to the direct write method.

Introduction

Additive manufacturing (AM) – and laser powder bed fusion (LPBF) in particular – is well known for its ability to construct geometric forms that would not be possible using standard manufacturing techniques [1-3]. This geometric versatility has inspired a design practice known as functionality integration – where multiple components are condensed to create a single part that performs all of the functions that were previously attributed to the individual components. While this practice can be quite useful in terms of weight reduction, part count reduction, and meeting spatial confinements; there are also serious drawbacks [4]. One of these drawbacks occurs in LPBF when different functions integrated into a single part have extremely different requirements (e.g. high fracture toughness on the interior and high hardness on the exterior), but the process can only sustain a single material [5]. This dilemma generally results in over-designing some areas of the part to compensate for the compromise in material choice. Over-designing can lead to decreased functional efficiency, increased weight, decreased fatigue life, etc. in LPBF parts. Creating methods to control the material composition spatially throughout a build would allow for designers to mitigate the negative effects and experience the full benefits of functionality integration.

The literature reports multiple attempts to expand LPBF processes into the multi-material regime. One approach is to simply switch out the powder feedstock for a different material at a certain point in the build [6, 7]. While this has been done successfully in some cases, it greatly increases the overall build time. Because of the time sacrifice, it is generally limited to a single, large composition change during the build. This discrete change in composition can be problematic. Materials with vastly different properties create extra residual stresses from thermal expansion and contraction during fabrication and poor adhesion at the inter-material surface due to poor wetting and insufficient mixing [7, 8]. Some studies have shown that adhesion can be

improved by remelting the inter-material zone multiple times to improve mixing between the dissimilar materials, but this adds even more time to the process [7]. In addition to quality concerns, this method is still limited to material change in one direction and few changes throughout the part.

Other research has been done on methods of three-dimensional variation of composition. Wei et al. [9] have implemented a process that uses a vacuum to remove base powder in select areas and a separate hopper and nozzle to deposit powders of different compositions in the excavated areas. This novel method has been shown to work with glass-metal, metal-metal, ceramic-metal, and metal-polymer systems and has shown significant improvement in terms of spatial control throughout all three dimensions [9-14]. The method of Wei et al. has the downside of allowing powder of different compositions that is not fused to remain in the powder bed and contaminate the unfused powder that would be recycled. Since powder recycling is one of the main factors that contributes to the economic feasibility of LPBF, this method significantly increases the cost of the overall process [15]. The other significant cost issue that is affected by this multi-material method is the increase in time necessary to complete each layer. Vacuuming out and replacing powder can more than double the overall process time that originally consisted of only powder spreading and laser scanning. Large composition changes in three dimensions present the same issues observed for large composition changes in one dimension.

New Approach to Multi-material Laser Powder Bed Fusion

Many of the issues that are present in these current multi-material LPBF (MM-LPBF) efforts could be mitigated or eliminated by using liquid or liquid-encased dopants as the means of altering composition in a way that does not significantly add to the build time. The nature of the LPBF process provides two distinct opportunities for the introduction of liquid dopant to the powder bed. The first of these opportunities occurs after a layer is fused by the laser but before the next layer of powder is spread. The second is just after the powder is spread but before the layer is fused.

In the first case, liquid dopant could be deposited on the solid substrate using either a direct write (controlled extrusion through an orifice) or droplet-based deposition method like inkjet printing (see Figure 1). The liquid would be dried either by the heat in the build chamber or using an exterior heat source (such as a lamp or the laser at low power) after which the next layer of powder would be spread. This method provides a distinct advantage of the dopant being covered by powder of the base material, which would reduce the amount of dopant that is evaporated or ejected as spatter during the fusing process. Since the dopant is initially concentrated in a specific area (between the powder and substrate) this may also affect the final location and dispersion of the dopant throughout the melt pool. Direct write can also be used with a wide range of suspension properties and has little risk of clogging in the nozzle. However, direct write can be slow since it is generally only used with a single nozzle.
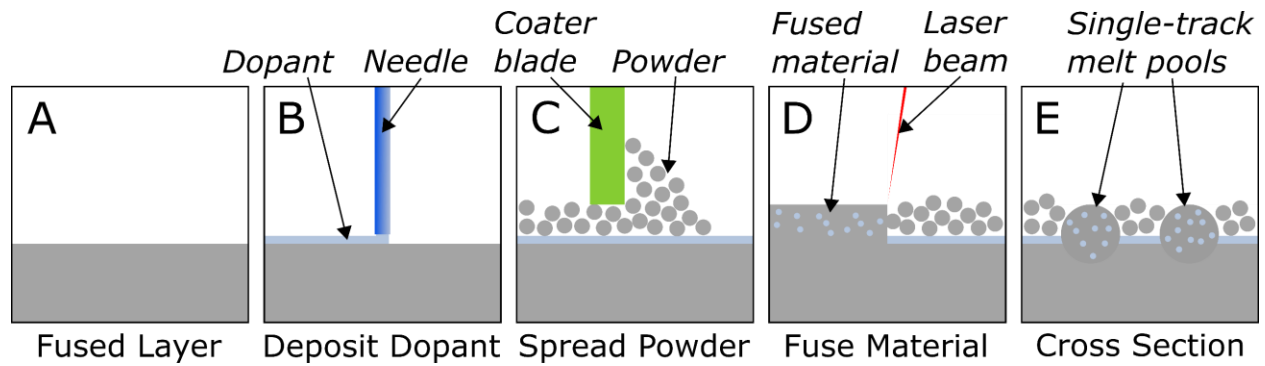
Figure 1 - Direct write liquid dopant deposition method. The liquid dopant is deposited using an open-tip needle directly onto the previous (fused) layer. Once the dopant is dry, the powder is spread over the top and the fusing process is carried out and the base and dopant materials are mixed.

In the second case, the powder layer would be spread and then the liquid dopant would be deposited into the spread powder before the layer is fused (see Figure 2). Deposition in this method could only be done using a droplet-based system like the inkjet printing technology used in binder jetting – another AM technique. An inkjet printhead could be mounted on the coater blade system to print while spreading the next layer of powder – minimizing the impact on the total build time.
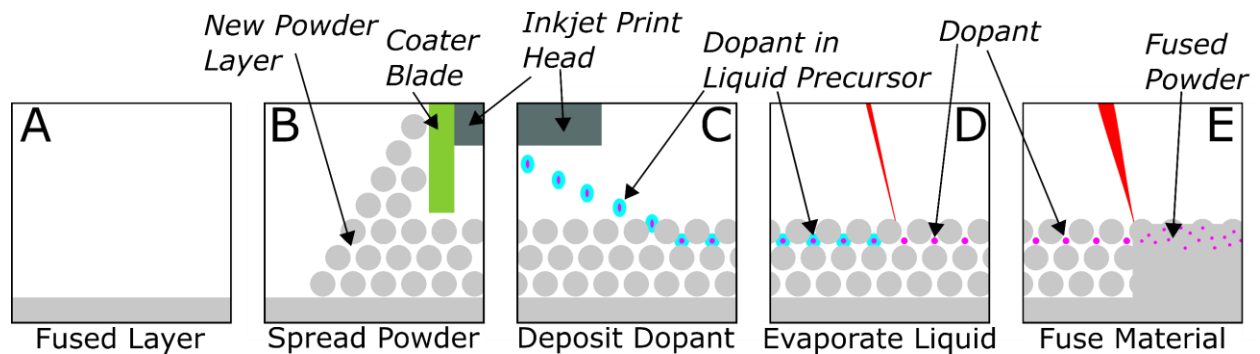

Figure 2 - Inkjet liquid dopant deposition method. After the powder is spread, liquid dopant is deposited into the powder in the form of micro-scale droplets from an inkjet printhead. Once the dopant and powder bed are dry, the fusing process is carried out.

This work focuses on evaluating the feasibility of depositing liquid dopants as part of the LPBF process by exploring the implications of exploiting the two deposition options described. These situations are replicated in a way that does not permanently alter the existing LPBF system. Direct write of a liquid dopant onto a solid substrate mimics the deposition onto a fused layer before the next layer of powder is spread, while inkjet deposition into a powder bed represents deposition after a powder layer is spread but before the layer is fused together. Simplified versions of these two methods are performed with careful observation of any requirements or outcomes that could significantly affect integration of the method to the LPBF process. Conclusions are made as to the deposition quality, integration feasibility, and system productivity of the two methods in relation to their application in LPBF.

Methods

Materials

Two dopant material systems were selected based on the availability of stable commercial suspensions and the potential for property enhancement in SS 316L. One material system that has previously been studied with LPBF is alumina (Al_2O_3) reinforcement in a stainless steel 316L matrix [16]. In this study, Li et al. showed that the addition of 1 to 3 $wt\%$ alumina to stainless steel processed using LPBF improved hardness in all cases and improved yield and tensile strengths in the case of 1-$wt\%$ alumina addition. While this study by Li et al., and most multi-material studies in LPBF, have been done using physically mixed matrix and additive powders, the property improvements shown demonstrate that the alumina/SS 316L material system is a useful material system for testing composition adjustment using alternative doping techniques.

Another material system of interest is zirconia (ZrO_2) reinforcement in a steel matrix. Koopmann et al. [7] showed that zirconia powder can be processed reasonably well using LPBF and that it can have good adhesion with steel when the interface between the two materials undergoes sufficient mixing during the laser processing. While their research was focused more on large composition changes, the good mixing between the two materials and processability of zirconia indicate that it could be a suitable test subject for feasibility of composition adjustment using alternative doping techniques.

In both the direct write and inkjet deposition methods, SS 316L powder (CL 20ES, Concept Laser, 29.9 μm, spherical) is used as the base material, to which either alumina or zirconia is added in the form of a water-based slurry using one of the two deposition methods described. The alumina slurry is Gamma B 0.05 μm Alumina from LECO with a 10 $wt\%$ concentration alumina with an added 10 $wt\%$ propylene glycol. The zirconia slurry is ZR100/20 from NYACOL with 20 $wt\%$ colloidal zirconia with a mean particle size of 100 nm. The alumina and zirconia concentrations were measured to be 10.6 and 25.4 $wt\%$ respectively. The LPBF machine used is a Concept Laser M2 Cusing Multilaser.

Direct Write

Direct write deposition describes a system in which a material is extruded directly onto a substrate through an orifice (see Figure 1 and Figure 3). The material creates a liquid bridge with the substrate that moves with the needle and leaves a liquid track behind. This technique would be difficult to apply to a powder bed as the fluid meniscus would likely move the powder during liquid deposition; however, it is suitable for deposition on a solid substrate. In the current study, the direct write deposition is applied to deposit alumina or zirconia slurry onto a solid plate made of SS 316L to simulate the case in which dopant is deposited on a previously fused layer.

A custom direct write system (see Figure 3) was used for printing [17-19]. The system uses a 3-axis CNC stage and a stepper motor to control the plunger of a syringe with an open-tip needle to deposit the slurry. The needle used was 25 gauge with a 0.305 mm inner diameter. The plate was leveled with respect to the x- and y-axis movement of the system and the needle was zeroed to the surface of the flat plate. Deposition was performed with the needle tip at a distance of 0.10 to 0.15 mm above the plate surface. Areas and lines were deposited at a flow rate of 0.0454

mm^3/mm while the needle traveled at speeds of 80 mm/s relative to the plate surface. Area depositions were performed in a concentric, rectangular pattern. The spacing between tracks was varied to control the total amount of slurry deposited in a given area. The dopant concentration in the slurries was also varied by adding distilled water to dilute the slurry to a predetermined concentration. The combination of these two adjustments was used to vary the overall dopant concentration amounts as described in Table 1 for the alumina depositions and Table 2 for the zirconia depositions.
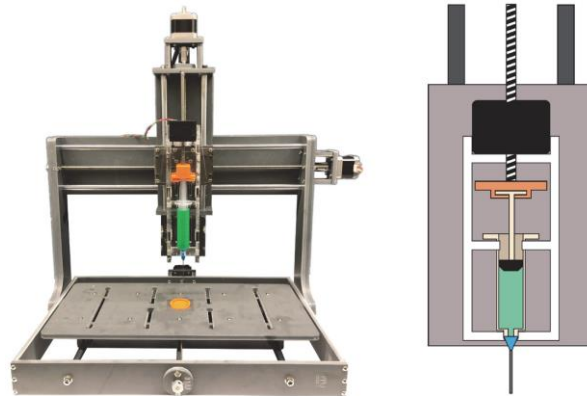

Figure 3 - Direct write deposition system (image from Romero et al. [19] used with permission). The three-axis stage controls the deposition location while the stepper motor above the syringe controls the rate of material ejection from the needle onto the substrate.

Table 1 - Deposition parameters and calculated deposition results for direct write deposition of alumina slurries over an area of 37 x 25 mm.

Area #	Slurry concentration ($wt\%$)	Volume deposited (mm^3)	Area density of alumina deposited ($\mu g/mm^2$)
1	3	100.28	3.166
2	2	100.28	2.120
3	1	100.28	1.064
4	0.5	100.28	0.533

Table 2 - Deposition parameters and calculated deposition results for direct write deposition of zirconia slurries over an area of 37 x 25 mm.

Area #	Slurry concentration ($wt\%$)	Volume deposited (mm^3)	Area density of zirconia deposited ($\mu g/mm^2$)
1	20	97.5	26.433
2	10	97.5	11.907
3	10	97.5	11.907
4	10	97.5	11.907

After the slurry was deposited, the plate was baked at 200 °C for 30 minutes to evaporate the remaining moisture and propylene glycol (boiling point ~ 190 °C) additive before installation to the LPBF machine. Using the LPBF machine's coater system and build chamber controls, a

layer of powder was spread over the dried alumina by adding 500 μm of powder and removing powder in 100 and 50 μm increments to get to a 50 μm powder layer. This was done to determine if the alumina deposits were stable during the powder coating step or if they would break down and contaminate the powder.

Direct write single-line depositions were also performed to investigate the difference between small- and large-area depositions. In these cases, the substrate was heated during deposition to a temperature of 50 °C rather than baking the substrate after deposition to simulate a heated build plate during the LPBF process.

Inkjet

The inkjet method is suitable for printing dopants into spread powder layers. While printing into powder can be challenging [20, 21], it is successfully done in both the binder jetting and multi jet fusion/high speed sintering commercial processes. In order to simulate dopant deposition onto loose powder, a solid SS 316L plate was used as a base onto which walls were built to create isolated pockets of powder. These pockets reduce the error in quantifying the amount of dopant deposited by limiting the area into which the dopant can spread. The pocket walls were built in the LPBF machine with a laser power of 370 W, a scan speed of 1350 mm/s, and a spot size of 130 μm. The walls were built by depositing a 25 μm layer of powder, fusing the pocket walls, depositing another 25 μm powder layer (50 μm total) and fusing the pocket walls again (see Figure 4). These 25 μm increments are smaller than typical to ensure total fusing of the pocket walls with the base plate so that each pocket was totally separate from the others. Once these pockets were built, the powder inside the pockets was left undisturbed while the plate was taken out of the LPBF machine and transported to the inkjet printing station.
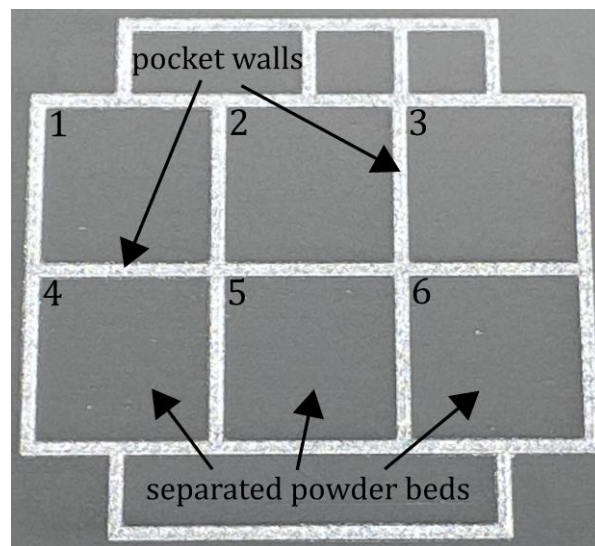

Figure 4 - Pockets walls printed 50 μm tall on substrate to separate powder beds of the same height. Powder beds before inkjet deposition are fairly uniform. Pocket walls and individual powder beds are labeled. Individual pocket labels are also included for future reference.

A simple inkjet setup (see Figure 5) was used to deposit colloidal zirconia slurry into the walled-off powder beds [20, 21]. This setup uses a pressurized chamber connected to a single, 80

μm-nozzle, piezo-electric, drop-on-demand print head (MicroFab Technologies, Inc.; Part # MJ-AB-01-80-8MX) controlled in coordination with the movements of the stages to create lines of consistently-spaced droplets. The nozzle released droplets at a rate of 1000 Hz while moving in the x-direction at a speed of 60 mm/s creating a droplet spacing of 60 μm. The plate was baked after deposition at 180 °C for 30 minutes to evaporate the liquid from the slurry. When multiple passes were necessary to achieve the desired concentration, the plate was baked between passes as well.
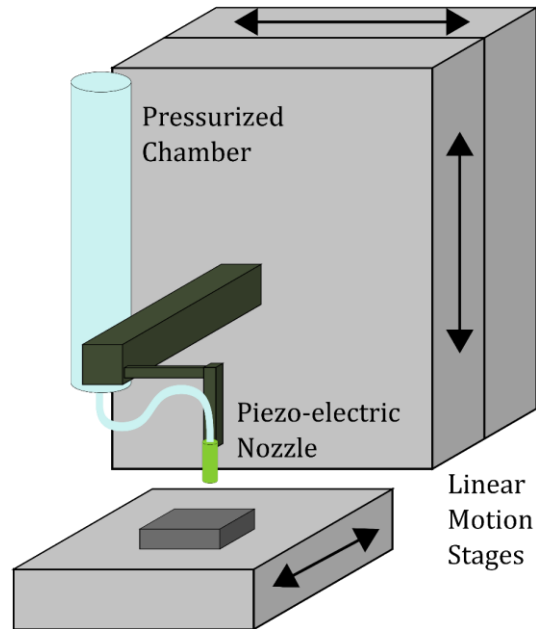

Figure 5 - Single-nozzle inkjet deposition system. The three axis stage controls the deposition location while the piezo-electric nozzle controls the droplet size and ejection frequency into the powder bed or onto the substrate.

Inkjet Calculations

The concentration of dopant in the powder bed was controlled by varying the line spacing and number of lines for each pocket (see Table 3). These parameters were chosen based on an estimate of how much dopant would be integrated into the melt pool during laser processing. Some of the values are purposefully higher than might be typically needed in order to test the upper limits of the deposition method.

Table 3 - Deposition parameters for inkjet deposition of zirconia slurry.

Pocket #	# of passes	# of lines / pass	Line spacing (mm)
1	3	1060	0.0226
2	3	774	0.0310
3	1	1506	0.0159
4	1	1506	0.0159
5	1	886	0.0271
6	1	290	0.0830

Droplet volume was measured by jetting the zirconia slurry in a stationary position for 10 minutes into a 5 mL beaker of known mass. The beaker was then baked at 180 °C for 30 minutes – leaving only the zirconia – and weighed again. Subtracting the original mass of the beaker from the mass of the beaker and zirconia gives the mass of zirconia deposited over the time interval (m_z). This can then be used to estimate the amount of slurry deposited (m_{sl}) by $m_{sl} = m_z/c$ where c is the zirconia concentration in the slurry. The number of droplets can be calculated as $n_d = t * f$ where t is the deposition time and f is the droplet frequency. The slurry mass and number of droplets can then be used to calculate the mass and volume of an average droplet (m_d and V_d respectively) by $m_d = m_{sl}/n_d$ and $V_d = m_d/\rho_{sl}$ where ρ_{sl} is the density of the slurry provided by the manufacturer (1.22 g/cm^3). The average amount of zirconia per droplet (m_{z_d}) can also be calculated as $m_{z_d} = m_z/n_d$ using the same values for m_z and n_d as above. Using these calculations, the droplets were measured to have a volume of about 0.145 $nL/droplet$ and to contain about 35.4 ng of zirconia in each droplet.

The droplet volume described above was used to calculate estimates of the amount of slurry/dopant deposited into the powder beds (see Table 4). Total volume was obtained by calculating the number of droplets in each line and multiplying by the number of lines for the deposition. The total saturation is the measure of the amount of space between powder particles that is filled by the slurry. The powder packing fraction was assumed to be 50%, which is typical for non-compacted powder beds [22]. An area density is also calculated by dividing the total mass of zirconia deposited over the area that it was deposited. This total mass of zirconia is obtained in similar fashion to the total volume by using the total number of droplets in a given deposition.

Table 4 - Predicted volume, saturation, and density calculations for the inkjet parameters mentioned in Table 3. Pocket numbers are defined in Figure 4.

Pocket #	Total volume deposited (mL)	Powder bed saturation (%)	Area density of zirconia deposited ($\mu g/mm^2$)
1	0.1794	1281.8	78.19
2	0.1309	935.4	57.06
3	0.0850	607.2	37.04
4	0.0850	607.2	37.04
5	0.0499	356.8	21.76
6	0.0163	116.5	7.11

Results and Discussion

The resulting deposits from the two deposition methods can be seen in Figure 6 and Figure 7. Since there are no quantitative metrics readily available to evaluate these deposition methods, qualitative visual observations of these resulting deposits are the basis for many of the claims as to the value of the two methods. Other observations were also made by the authors during the deposition processes that are included in the ensuing discussion.

Figure 6 - Dried alumina (left) and zirconia (right) deposits performed using direct write deposition.
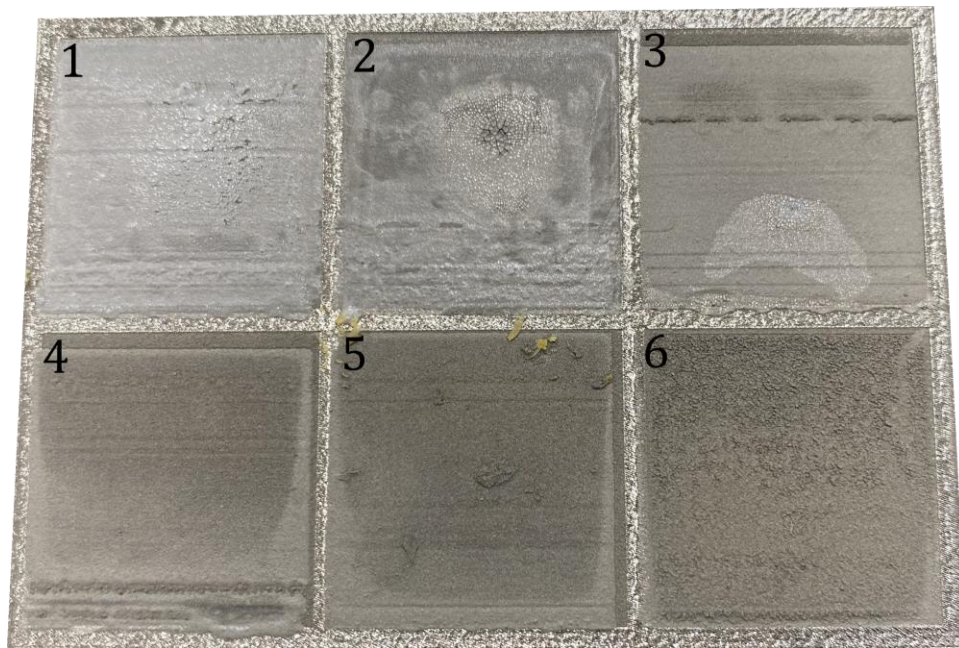

Figure 7 - Resulting deposits from inkjet deposition method into small, enclosed powder bed using various dopant densities.

Three criteria were selected to evaluate and compare the two deposition methods. These criteria are deposition quality, integration feasibility, and system productivity. Deposition quality refers to the uniformity of the deposited material as well as the accuracy of quantity and location of the deposited material. Irregularities, non-uniformities, and inaccuracies would diminish the value that a deposition method could provide. Integration feasibility refers to how well the deposition method could be integrated into the LPBF process. This includes reliability and repeatability of the deposition method. It also involves any ways in which the deposition method would disrupt, interfere with, or otherwise negatively impact the LPBF process as a whole. System productivity refers to the overall value that a combined deposition/LPBF system would provide.

This includes build time increases, feasible concentration ranges, and other things that would need to be considered when implementing the full deposition/LPBF system. The direct write and inkjet deposition methods are both evaluated according to these three criteria by observing various characteristics of the deposition processes in action as well as qualities of the resulting dopant deposits.

Deposition Quality

Direct Write

The quality of the direct write process was mostly impacted by inconsistencies observed during deposition and in the resulting dopant structures after drying.

The first non-uniformity was observed in moments when the needle tip was too far from the deposition surface. In these instances, the slurry would "skip" small sections of the deposition area because the slurry would build up around the edge of the needle instead of wetting and depositing on the substrate. The skipping would eventually end when the size of the slurry bead on the needle was large enough to make contact with slurry that had already been deposited or the substrate itself. Areas where skipping occurred can easily be seen in recently-deposited areas as small holes or lines in the deposition areas (see Figure 8 - Photos of liquid zirconia slurry in different concentrations shortly after deposition by direct write. Some instances of "skipping" are indicated by red arrows. A large area in the bottom right deposition did not deposit due to silicone contamination on the surface that altered the plate wetting.).

Figure 8 - Photos of liquid zirconia slurry in different concentrations shortly after deposition by direct write. Some instances of "skipping" are indicated by red arrows. A large area in the bottom right deposition did not deposit due to silicone contamination on the surface that altered the plate wetting.
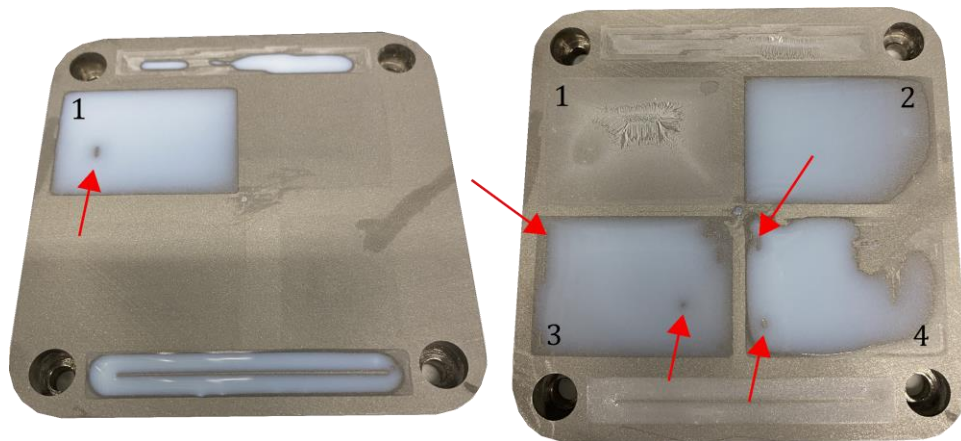
Skipping was also observed in single-line depositions (see Figure 9). The effect was slightly different, however, as there were generally no nearby depositions that could be used to reestablish contact between the slurry in the needle and the substrate surface. When this happened, much more slurry built up on the needle tip than during the area depositions. This resulted in larger sections of the deposition area without dopant and large bead-like areas shortly after the blank sections.
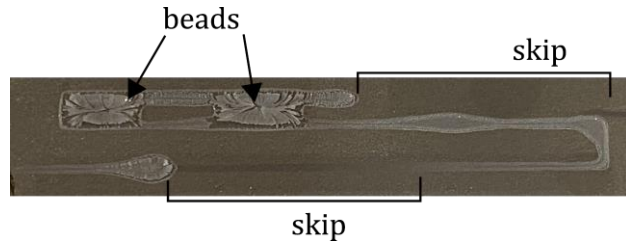
Figure 9 - Direct write deposition of zirconia in single-track lines. Some instances of "skipping" are indicated by red brackets. Beads resulting from the skipping are indicated with red arrows.

Another type of non-uniformity was observed when the dopant material moved toward the center of the deposition areas during the drying/baking stage. As the edges of the deposition areas began to dry, the solid particles were transported inward ahead of the solid/liquid interface [23]. The literature attributes this type of capillary push to the decreasing height of the liquid wedge near the contact line [24, 25]. The result was a higher-concentration area in the center of the deposition area with low dopant concentrations near the edges (see Figure 10). While this trend was consistent for all of the direct write depositions, the magnitude of the resulting dopant concentration disparity varied with the input slurry concentration. When the slurries were diluted to lower concentrations, less of a gradient was observed throughout the deposition area.

Figure 10 – Recently-deposited liquid alumina slurry diluted to different concentrations. Each image shows the deposition of a unique concentration to a different quadrant on the substrate. Left to right: 3 wt%, 2 wt%, 1 wt%, and 0.5 wt% slurry. Dopant agglomeration near the centers of the deposition areas is observed as more white (alumina) than the exterior regions of the depositions.

One last concern about the quality of the direct write method is the structure and stability of the resulting dopant deposit – especially in the highly-concentrated regions. In the alumina deposits, the highly-concentrated centers were quite stable despite some small cracks. The zirconia deposits, however, formed extremely fragile, highly discontinuous structures in their centers that delaminated from the substrate in most cases (see Figure 6). These structures would be likely to break and move under almost any application of force. Since this structure fragility was only seen in the zirconia direct write depositions, this can be categorized as a reflection on the properties of the slurry/dopant and the drying conditions.

Overall, the deposition quality of the direct write method is not promising as it is non-uniform and can produce structurally unsound deposits in the case of zirconia dopant.

Inkjet

While the inkjet deposition method has the potential to have great uniformity, there are also many opportunities for error. In general, the samples with dopant deposited using this method are fairly uniform (see pockets 3, 4, and 5 in Figure 11) as long as simple errors can be avoided. One of these errors is clearly seen near the bottom of pocket 4 and just above the center of pocket 3. In these cases, the nozzle was clogged temporarily during the deposition resulting in a few missed lines where dopant should have been deposited. Another error seen in pocket 5 is contamination from an outside source as flakes of residue material fell from the nozzle structure into the pocket during deposition. These errors all affect the uniformity of the resulting deposition; however, they could be resolved with a more controlled inkjet system commonly used in industrial applications.
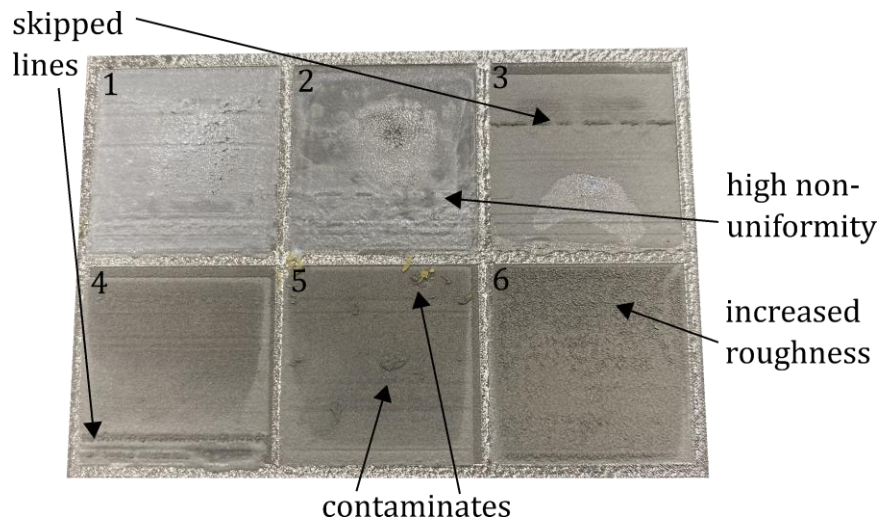

Figure 11 - Zirconia-doped powder beds at different concentrations with pocket 1 being the highest concentration and pocket 6 being the lowest (see Table 4 for detailed concentration estimates). Contaminates and skipped lines are the result of user-error during deposition while increased roughness and non-uniformity of dopant concentration are important results that will impact the LPBF process.

While the mid-range depositions appear uniform, the higher-density depositions (see pockets 1 and 2 in Figure 11) show more variance in the uniformity of the dopant concentration throughout the pocket. This is due to the increased movement of the liquid and powder during the deposition stage. The greater amount of liquid in the pocket created a pool of liquid, in which the 316L powder particles could flow.

The uniformity of the inkjet method can be somewhat limited in the higher range of saturations; however, increasing the dopant concentration in the slurry or depositing the material in multiple passes with drying between passes could expand the feasible range of doping deposits.

Integration Feasibility

Direct Write

In practice, there are a few things that would need to be considered before implementing the direct write method in an LPBF system.

The first of these is the needle tip distance from the surface. During the direct write operation, it was observed that the skipping mentioned above could be avoided by keeping the tip of the needle within about 0.15 *mm* of the substrate surface during deposition. This requires an extremely flat substrate which is not always the case with built layers in the LPBF process. During the depositions, it was noted that little to no skipping occurred when the substrates were level to within about 0.05 *mm*.

The incorporation of a direct write system into an LPBF machine would also require significant modifications. This would entail an additional motion axis for the nozzle to move in the direction perpendicular to the coater blade or two motion axes if the system moves independent from the coater system. A vertical motion axis may also be warranted to ensure that the nozzle tip does not come in contact with the metal powder at any point in the process and that it can be lowered to the correct height as mentioned previously.

Another important consideration is whether the dopant will contaminate the powder that will not be fused as part of the final build. The delaminated flakes of dried zirconia slurry would be broken off during powder spreading and could travel to almost any part of the build chamber. This would be problematic as the composition could be changed in the wrong locations within the part, unfused powder could be contaminated, and powder flowability could decrease due to the different shape and size of the zirconia inclusions. However, this problem is specific to the properties of the dopant. The plate with alumina depositions was inserted into the LPBF machine and powder was spread over the top. After removing the plate and clearing the powder, it was determined that the powder spreading process did not cause any visible physical damage to the deposited alumina.

Powder contamination could also be a concern when the dopant is still in liquid form. If the liquid in the slurry does not evaporate before the next layer of powder is spread, the powder could be contaminated as mentioned above. The moisture could also severely limit the flowability of the powder or even cause build-ups on the coater blade. Both of these cases could initiate the formation of defects that would propagate through multiple layers if not the entire build [26-28].

Inkjet

There are a few things that were noted in the inkjet process that may affect the way it is implemented in LPBF applications.

One of these observations was the dramatic change in color in the higher-density depositions. While all of the depositions did show some change in color, the change in pockets 1 and 2 were the most pronounced. This may be due to the dopant being present on the top surface of the powder bed at higher concentrations compared to the other depositions. This is of particular importance for LPBF because the added material being on top of the material could change the effective absorptivity of the powder bed. This change would require a shift in processing parameters to achieve the same part quality.

Another feature that could impact the LPBF process is the powder bed roughness observed in pocket 6 (see Figure 11). In binder jetting, this increase in roughness has been described as a first layer phenomenon that occurs when the droplets are too widely spaced [29]. This can cause

poor lamination throughout the first few layers in binder jetting. Similarly, in LPBF, increased roughness in one layer can cause balling and other defects in subsequent single-track scans or fused layers and can propagate throughout the part [26-28]. This could prove prohibitive to low-saturation depositions using the inkjet method; however, slurries or solutions with lower dopant particle densities could be used to achieve smaller composition changes while maintaining the same saturation levels.

While these effects on the LPBF process may require some adjustment, they are not prohibitive as other processes (such as binder jetting) have successfully addressed them through printing parameter adjustments [20, 21, 29].

Inkjet printheads can also be fitted across a wide span and could easily cover the entire width of the coater blade. This would make it so that no additional motion axis is required for incorporation into the LPBF system.

System Productivity

Direct Write

While using liquid dopants to alter composition may be quite attractive in an LPBF setting, the benefits of the method being used must outweigh the associated costs to make a reasonable claim at increasing value.

The main cost that this method incurs is the extra time that it will take. Since the deposition step cannot occur simultaneous to any of the other LPBF process steps, every layer where dopant is needed would take considerably longer to complete. This time addition could be in the range of a few seconds to a few minutes for each layer depending on the traverse speeds, the amount of dopant to be deposited, and the area over which it was to be deposited. The dopant then also needs to dry before continuing – to avoid introducing moisture to the delicate powder process as mentioned above. This wait could add more seconds or minutes onto each layer time depending on the size and shape of the deposits.

The benefits are also limited by the non-uniformity of the resulting dopant deposits. In order to maintain a somewhat uniform deposition, the direct write method as performed in this study would be limited to less than $0.6 \ \mu g/mm^2$ of alumina (or $0.3 \ wt\%$ of the deposited material when measured with a $50 \ \mu m$ layer of powder) for any area depositions. While this may be useful to alter some properties, it is on the low side of small composition change. Studies have shown that useful small composition changes are generally between 1 and 5 $wt\%$ for dispersion strengthening [16, 30]. However, the amount of dopant required to affect other changes in a material may be significantly higher.

In this case, the added time costs and small concentration range are extremely limiting when considering implementation of a direct write deposition system into a LPBF process.

Inkjet

The inkjet system has some clear advantages over the direct write system. The added time cost for this method will be close to nothing. Since inkjet printhead arrays can be scaled to perform

at very fast speeds and the printhead can operate simultaneous to the powder spreading, the deposition step will add very little if any time to the overall process. Considerations may need to be made for drying the liquid dopant; however, a heated build chamber could reduce that time cost significantly as well.

Though there are many benefits to using an inkjet deposition system with LPBF, there are some limitations as well. One specific limitation found during this study is that the alumina slurry did not work in the inkjet setup. With the small-aperture piezo-electric nozzles that were used with the inkjet system, a 5.00 μm filter was used to keep larger particles from damaging the nozzles. This filter made it impossible for the alumina slurry to pass through the system, meanwhile the zirconia slurry had no problems. This illustrates the need for careful preparation of the dopant to be used with an inkjet deposition system.

Generally, the inkjet deposition system has the potential to add significant value to the LPBF process. The problems and limitations can be addressed if the property enhancements are sufficient.

Conclusions

Overall, inkjet printing is a better option for liquid-dopant deposition in LPBF because of its superior uniformity, high resolution, minimal time addition to the process, and its history of use with powder beds (e.g. binder jetting). The direct write method could be beneficial in specific circumstances (e.g. single tracks of dopant), but would be much more difficult to implement across the rough surfaces often encountered in LPBF. The only clear advantage that the direct write method could claim over inkjet deposition is that the dopant is underneath the powder and would have a minimal effect on laser absorption. The inkjet method can deposit liquid dopants in concentrations between about 10 and 40 $\mu g/mm^2$ while the direct write method is limited to less than 0.6 $\mu g/mm^2$ for large areas. Choice of material that is suitable for the different methods is of paramount importance as zirconia proved to not be useful in the direct write method while the alumina slurry could not be used in inkjet printing. This limitation may be overcome by using inks that are formatted specifically for inkjet printing.

References

[1] A. du Plessis, C. Broeckhoven, I. Yadroitsava, I. Yadroitsev, C.H. Hands, R. Kunju, D. Bhate, Beautiful and Functional: A Review of Biomimetic Design in Additive Manufacturing, Addit Manuf 27 (2019) 408-427.

[2] A. Kover, Transformation in 3D: How a Walnut-Sized Part Changed the Way GE Aviation Builds Jet Engines, GE, GE Reports, 2018.

[3] J.O. Milewski, On the Road to AM, Additive Manufacturing of Metals: From Fundamental Technology to Rocket Nozzles, Medical Implants, and Custom Jewelry, Springer International Publishing, Cham, 2017, pp. 35-48.

[4] D. Bockin, A.M. Tillman, Environmental assessment of additive manufacturing in the automotive industry, J Clean Prod 226 (2019) 977-987.

[5] I.M. El-Galy, B.I. Saleh, M.H. Ahmed, Functionally graded materials classifications and development trends from industrial point of view, SN Applied Sciences 1(11) (2019).

[6] V.K. Nadimpalli, T. Dahmen, E.H. Valente, S. Mohanty, D.B. Pedersen, Multi-material additive manufacturing of steels using laser powder bed fusion, euspen's 19th International Conference & Exhibition, The European Society for Precision Engineering and Nanotechnology, 2019, pp. 240-243.

[7] J. Koopmann, J. Voigt, T. Niendorf, Additive Manufacturing of a Steel–Ceramic Multi-Material by Selective Laser Melting, Metallurgical and Materials Transactions B 50(2) (2019) 1042-1051.

[8] A.G. Demir, B. Previtali, Multi-material selective laser melting of Fe/Al-12Si components, Manufacturing Letters 11 (2017) 8-11.

[9] C. Wei, L. Li, X.J. Zhang, Y.H. Chueh, 3D printing of multiple metallic materials via modified selective laser melting, Cirp Ann-Manuf Techn 67(1) (2018) 245-248.

[10] Y.-H. Chueh, C. Wei, X. Zhang, L. Li, Integrated laser-based powder bed fusion and fused filament fabrication for three-dimensional printing of hybrid metal/polymer objects, Addit Manuf 31 (2020) 100928.

[11] C. Wei, Y.-H. Chueh, X. Zhang, Y. Huang, Q. Chen, L. Li, Easy-To-Remove Composite Support Material and Procedure in Additive Manufacturing of Metallic Components Using Multiple Material Laser-Based Powder Bed Fusion, Journal of Manufacturing Science and Engineering 141(7) (2019) 1.

[12] C. Wei, H. Gu, X. Zhang, Y.-H. Chueh, L. Li, Hybrid ultrasonic and mini-motor vibration-induced irregularly shaped powder delivery for multiple materials additive manufacturing, Addit Manuf 33 (2020) 101138.

[13] C. Wei, Z. Sun, Q. Chen, Z. Liu, L. Li, Additive Manufacturing of Horizontal and 3D Functionally Graded 316L/Cu10Sn Components via Multiple Material Selective Laser Melting, J Manuf Sci E-T Asme 141(8) (2019).

[14] X.J. Zhang, C. Wei, Y.H. Chueh, L. Li, An Integrated Dual Ultrasonic Selective Powder Dispensing Platform for Three-Dimensional Printing of Multiple Material Metal/Glass Objects in Selective Laser Melting, J Manuf Sci E-T Asme 141(1) (2019).

[15] I. Gibson, D. Rosen, B. Stucker, Powder Bed Fusion Processes, in: I. Gibson, D. Rosen, B. Stucker (Eds.), Additive Manufacturing Technologies, Springer New York, New York, NY, 2015, pp. 107-145.

[16] X. Li, H.J. Willy, S. Chang, W. Lu, T.S. Herng, J. Ding, Selective laser melting of stainless steel and alumina composite: Experimental and simulation studies on processing parameters, microstructure and mechanical properties, Materials & Design 145 (2018) 1-10.

[17] T.E. Greenwood, Silicone 3D Printing Processes for Fabricating Synthetic, Self-Oscillating Vocal Fold Models, Brigham Young University, 2020.

[18] T.E. Greenwood, S.E. Hatch, M.B. Colton, S.L. Thomson, 3D Printing Low-Stiffness Silicone Within a Curable Support Matrix, Addit Manuf (2020) 101681.

[19] R.G.T. Romero, M.B. Colton, S.L. Thomson, 3D-Printed Synthetic Vocal Fold Models, Journal of Voice (2020).

[20] T. Colton, N.B. Crane, Influence of droplet velocity, spacing, and inter-arrival time on line formation and saturation in binder jet additive manufacturing, Addit Manuf 37 (2021) 101711.

[21] T. Colton, J. Liechty, A. McLean, N. Crane, Influence of Drop Velocity and Droplet Spacing on the Equilibrium Saturation Level in Binder Jetting, SFF Symposium, 2019.

[22] K.M. Fan, K.W. Wong, W.L. Cheung, I. Gibson, Reflectance and transmittance of TrueFormTM powder and its composites to CO_2 laser, Rapid Prototyping Journal 13(3) (2007) 175-181.

[23] R.W. Balluffi, S.M. Allen, W.C. Carter, Kinetics of materials, John Wiley & Sons2005.

[24] D. Mampallil, H.B. Eral, A review on suppression and utilization of the coffee-ring effect, Advances in Colloid and Interface Science 252 (2018) 38-54.

[25] B.M. Weon, J.H. Je, Capillary force repels coffee-ring effect, Physical Review E 82(1) (2010).

[26] J.C. Snyder, K.A. Thole, Understanding Laser Powder Bed Fusion Surface Roughness, Journal of Manufacturing Science and Engineering 142(7) (2020) 1-37.

[27] R. Li, J. Liu, Y. Shi, L. Wang, W. Jiang, Balling behavior of stainless steel and nickel powder during selective laser melting process, The International Journal of Advanced Manufacturing Technology 59(9-12) (2012) 1025-1035.

[28] D. Gu, Y. Shen, Balling phenomena in direct laser sintering of stainless steel powder: Metallurgical mechanisms and control methods, Materials & Design 30(8) (2009) 2903-2910.

[29] T. Colton, The Impact of Inkjet Parameters and Environmental Conditions in Binder Jetting Additive Manufacturing, Department of Mechanical Engineering, Brigham Young University, Thesis and Dissertations, 2021.

[30] R.L. Klueh, J.P. Shingledecker, R.W. Swindeman, D.T. Hoelzer, Oxide dispersion-strengthened steels: A comparison of some commercial and experimental alloys, Journal of Nuclear Materials 341(2-3) (2005) 103-114.